JOURNAL OF THE ROYAL SOCIETY Interface

Cellular automata and integrodifferential equation models for cell renewal in mosaic tissues

J. M. Bloomfield, J. A. Sherratt, K. J. Painter and G. Landini

J. R. Soc. Interface published online 7 April 2010
doi: 10.1098/rsif.2010.0071

JOURNAL OF THE ROYAL SOCIETY Interface

FirstCite® e-publishing

J. R. Soc. Interface
doi:10.1098/rsif.2010.0071
Published online

Cellular automata and integrodifferential equation models for cell renewal in mosaic tissues

J. M. Bloomfield[1,*], J. A. Sherratt[1], K. J. Painter[1] and G. Landini[2]

[1]*Department of Mathematics and the Maxwell Institute for Mathematical Sciences, School of Mathematical and Computer Sciences, Heriot Watt University, Edinburgh, EH14 4AS, UK*
[2]*School of Dentistry, College of Medical and Dental Sciences, University of Birmingham, St Chad's Queensway, Birmingham, B4 6NN, UK*

Mosaic tissues are composed of two or more genetically distinct cell types. They occur naturally, and are also a useful experimental method for exploring tissue growth and maintenance. By marking the different cell types, one can study the patterns formed by proliferation, renewal and migration. Here, we present mathematical modelling suggesting that small changes in the type of interaction that cells have with their local cellular environment can lead to very different outcomes for the composition of mosaics. In cell renewal, proliferation of each cell type may depend linearly or nonlinearly on the local proportion of cells of that type, and these two possibilities produce very different patterns. We study two variations of a cellular automaton model based on simple rules for renewal. We then propose an integrodifferential equation model, and again consider two different forms of cellular interaction. The results of the continuous and cellular automata models are qualitatively the same, and we observe that changes in local environment interaction affect the dynamics for both. Furthermore, we demonstrate that the models reproduce some of the patterns seen in actual mosaic tissues. In particular, our results suggest that the differing patterns seen in organ parenchymas may be driven purely by the process of cell replacement under different interaction scenarios.

Keywords: chimera; chimaera; Blaschko lines; cellular automata; organ parenchyma; voter model

1. INTRODUCTION

Proliferation is a fundamental cellular process, forming the basis of renewal in all higher organisms. It has an important role in many situations, including embryogenesis and tissue maintenance, although the extent to which it is a driver for such multi-cellular processes is not known. Cellular proliferation is modulated by cell signalling. This may be contact-dependent, requiring cells to physically touch each other, or it may involve longer range processes (Webb & Owen 2004; Graham & van Ooyen 2006). Once a cell has received a proliferation signal, it produces a daughter cell of its own type.

The question of how the decision to proliferate is made has appeared in relation to multiple biological problems. One such, which we will concern ourselves with here, is that of mosaicism. Mosaic tissues are composed of two or more genetically distinct cell types, and the mosaic patterns produced by this mix of cells are witnessed in many scenarios. For example, certain human diseases involving mutations early in embryogenesis can exhibit macroscopic patterns in skin along the so-called Blaschko lines, which are thought to indicate the limits between different proliferating cell clones (Happle 2006). Mosaic patterns also arise in all females due to X-chromosome inactivation: females carry two X-chromosomes, one of which is inactivated early in embryogenesis to prevent overexpression of X-chromosome genes. This inactivation process is known as Lyonization (Lyon 1961), and as the inactivation is passed on to daughter cells, it leads to females being a mix of two different cell types, with either the paternal or maternal X-chromosome active. This inactivation may also be related to Blaschko lines becoming visible in some pathological conditions in females, again following boundaries between the two cell types (Happle 2006).

Experimentally, mosaicism can be explored through the use of chimaeras. Chimaeric animals are individuals that have four or more parents. They are created by the fusion of distinguishable embryos, or by transgenic techniques (incorporating certain cell markers into one of the embryonic cells). Experimentalists have used chimaeras to consider the fate of cell clones, the spread and effect of certain mutations, and the cellular composition of different organs in parenchyma growth (see Ng & Iannaccone 1992; West 1998 for more details).

*Author for correspondence (jmb7@hw.ac.uk).

Received 9 February 2010
Accepted 16 March 2010

A better understanding of exactly how mosaic patterns arise would provide an important contribution to the problems outlined above. As chimaera experiments in particular have been so successful in the exploration of mosaics, we discuss them in detail here, with particular reference to their relevance for the growth and maintenance of organ parenchyma (i.e. the tissue that is essential to organ function). Although the patterns formed in chimaeras during the development of organ parenchymas can only be viewed after their creation, they do provide a tool against which hypotheses for growth and maintenance can be tested. *In situ* analysis of chimaeras has revealed different complex patterns in different organs. In the rodent liver, for example, cell lines appear to mix randomly, whereas the adrenal cortex produces radial stripes of cell lineages. It has been suggested that mosaics observed in the liver could be caused by cells proliferating randomly (Khokha *et al.* 1994; Iannaccone *et al.* 2002) while in the adrenal cortex, the placement of daughter cells may be biased centripetally (Iannaccone & Weinberg 1987; Landini & Iannaccone 2000; Iannaccone *et al.* 2002).

The suggestion that two very different organ parenchyma mosaics could both be caused by differences in proliferation (modulated, perhaps, by cellular contact, Landini & Iannaccone 2000), opens up the possibility that all organ parenchyma growth might be guided by cell proliferation and renewal alone, as opposed to other factors such as cell migration (Morley *et al.* 1996). Until experimental techniques can be improved, a theoretical approach such as mathematical modelling provides a valuable method of testing different hypotheses. Before we consider our own model, we discuss the models seen in the current literature that consider chimaera experiments, and also those that look at more general issues concerning the regulation of cell renewal by the local environment.

Few models have been produced to specifically describe the chimaera experiments above; those that have are mainly cellular automata (CA). A population of cells is arranged on a grid with rules imposed to govern the movement, growth and death of each cell according to both the position of neighbouring cells and the age of the cell itself. These models reproduce various chimaeric patterns (Landini & Iannaccone 2000), but only explicitly consider the proliferation hypothesis, not the cell migration/proliferation hypothesis. A CA model for an experiment involving chick and quail cells in the intestine, very similar to the chimaeras already discussed, is explored in Simpson *et al.* (2007*a*). This paper considers both cell migration and proliferation, and the results of the CA are successfully matched to that of experimental data; it is also noted that the dynamics produced by the CA match those of the Fisher partial differential equation (see Murray 1989, vol. I, ch. 11), demonstrating a successful multiscale modelling process. In Simpson *et al.* (2006, 2007*b*), a general continuous mathematical model of cell invasion is created and validated with experimental data. Proliferation is shown to be the key mechanism in driving the invasion process.

In this paper we take both a discrete and a continuous approach. It is possible to link discrete and continuous models formally as is done, for example, in the liver growth model of Green *et al.* (submitted), but we do not attempt that here as there is no relevant experimental data available that would call for such a link. Instead we take a more phenomenological approach. Following on from the successful discrete models of Khokha *et al.* (1994) and Landini & Iannaccone (2000), and the experimental work discussed above (particularly the observations made by both Simpson *et al.* (2006) and Landini & Iannaccone (2000) regarding the importance of cell proliferation), we assume cell proliferation, or more precisely, cell renewal to be the driving force for the dynamics. Through modelling, we can exclude all other factors from the system, such as mechanical effects, cell ageing, migration, etc., thereby testing whether cell renewal on its own is able to create the empirically observed variety of mosaics. We explore two different replacement mechanisms, both of which incorporate the effect of neighbouring cells on cell renewal. Although our model is designed for the investigation of organ parenchymas, it is also applicable to a range of other cell replacement problems.

Section 2 outlines the conceptual framework behind our theoretical models, and §2.1 considers the discrete CA model for a cell renewal problem based on chimaera experiments. We then begin §2.2 by describing the derivation of the continuous model, which has two slightly different versions, and which is the main focus of this paper. We consider the behaviour of the model for cells in two space dimensions in §3, and demonstrate the ability of the model to form organ parenchyma mosaics as witnessed in both the adrenal cortex and the liver, as well as showing some more general results. In §4 we discuss our findings, and go on to discuss another biological application for the model: that of Blaschko lines. We end by discussing potential directions for future work.

The key finding of this work is that, by changing the way in which the local cellular environment regulates cell renewal in our models, we can radically alter the patterns produced. In cell renewal, proliferation of each cell type may depend linearly or nonlinearly on the local proportion of cells of that type, and these two possibilities produce very different patterns. This observation offers possible answers to the question of why different organ parenchymas produce different mosaics, as observed in chimaera experiments and discussed in this section. Our results suggest that these various patterns may be created by different cell replacement scenarios mediated by different reactions to the local cellular environment.

2. MODELLING CHIMAERA EXPERIMENTS

Chimaera experiments are used to explore tissue dynamics by observing patterns generated by subpopulations of cells. These subpopulations are effectively identical apart from a marker that enables them to be distinguished.

We outline two conceptual models, both of which are based on biological hypotheses of cell renewal. Of course, various other conceptual models could also be suggested, but as the mechanism that regulates cell renewal in various organs has not been fully elucidated, we choose two different but probable mechanisms here. First, we suggest that a mix of two differently marked, but otherwise identical cell types die and are reborn according to a 'voting' principle: a cell dies randomly, and is replaced by a cell of whichever type is in the majority in its immediate neighbourhood. If there is an even mix of neighbouring cell types, replacement is allocated randomly. We call this the majority conceptual model, and it is akin to the idea that proliferation is biased towards the cell type which is in the majority locally. Although we are not aware of specific data supporting this hypothesis in cell renewal, such community effects are well documented in the regulation of other cell behaviours (Standley *et al.* 2001), and certainly would be a probable candidate for renewal in cells that communicate through local mechanisms such as juxtacrine signalling.

A second scenario dictates that a cell is replaced by the same type as a cell selected randomly from those in its immediate neighbourhood. This is the single-cell conceptual model, and represents basic cell proliferation whereby empty space is filled via the division of a cell in its immediate neighbourhood.

We model these concepts in two dimensions, thereby considering a monolayer of cells. For both of these scenarios, we assume that the population of cells stays constant, i.e. that death and birth are instantaneous. This means that we are modelling a process of tissue homoeostasis, as opposed to tissue growth. We further assume that there is no empty space, which allows us to think of this model as a one population model: a cell is either of one type or the other. Furthermore, since the two populations are only differentiated by a marker but are otherwise the same, we assume that both birth and death rates in the two populations are the same. Both the majority and the single-cell conceptual models provide a simplified representation of a synthetic chimaera, and we simulate them as such to investigate the emerging patterns.

2.1. The cellular automata approach

Individual-based models are very well established and come in many different formats (see Anderson *et al.* 2007 for a review). For our purposes it is sufficient to use a very simple CA model, even though more sophisticated forms are available. CA have been applied to many biological applications as their discrete form lends itself naturally to the modelling of biological cells. We set up two CA 'voter' models according to the conceptual models outlined above (see Liggett 1985, ch. 5 for a more general description of voter models). The processes for the two models are outlined in figure 1.

While the algorithms in figure 1 describe asynchronous random choice updating (Schönfisch & de Roos 1999), we have also implemented a synchronous updating method, meaning that all grid squares across the lattice are updated simultaneously, with new values calculated according to their neighbours at the previous time-step. No qualitative difference in results from the two updating algorithms is observed, beyond that of time scale. The simulations illustrated here all employ asynchronous updating.

Bearing in mind our biological application to chimaera experiments, we explore initial conditions of two cell types evenly mixed across the grid for each of the conceptual models. For the majority conceptual model the end result is either domination by a single cell type across the grid (figure 2*a–d*), or a split domain in the form of one large block of each cell type (figure 2*e–h*). This result is seen both for our choice of neighbourhood (an eight-cell 'Moore' neighbourhood), and in a more preliminary simulation study using a four-neighbour 'von-Neumann' neighbourhood, which involves just cells that share a complete edge with the empty site. The significance of the von Neumann neighbourhood is that it is the predominant formalism in the extensive literature on the so-called threshold voter models, which are otherwise similar to our majority conceptual model. In the threshold-2 voter model, cells switch type at a given rate if at least two (out of four) neighbours are of the opposite type (Cox & Durrett 1991). While this is not quite the same as our majority model, both models do have the possibility of switching only when half of the neighbours are of opposite type. Cox & Durrett (1991) conjecture that such a model will evolve to all of either one cell type or the other dominating across the domain, depending on which cell type has the greater initial density, with a density of precisely $\frac{1}{2}$ being the critical value at which the switch between these two scenarios occurs. This is consistent with our observation that with initial conditions of two cell types mixed approximately evenly across the grid, we see either the steady-state solution of all one species, all the other, or split between the two.

For the single-cell conceptual model we do not observe the system evolving to a single cell type, even when the simulations are run on a long time scale. Rather, cell types agglomerate in a constantly changing pattern (figure 2*i–l*), forming solid groups. We see this over long time scales (we investigated up to $t = 10^8$, and still saw this spatially unstable movement). Again, preliminary investigations show no qualitative difference between simulations using a von Neumann neighbourhood and those carried out on a Moore neighbourhood, making the literature on voter models relevant. The literature states that for models similar to this, clustering is the expected result, i.e. cell types group into larger and larger blocks, until the solution runs to a single species steady state as $t \to \infty$ with probability 1 (Cox & Durrett 1991; see also Cox & Griffeath 1986; Dornic *et al.* 2001). We do not see this end state; rather, our simulations show (in figure 2*i–l*) the initial clustering process where the two cell types form larger solid blocks as time increases. The much longer time scale over which a single species emerges is not biologically relevant.

These results show that the different types of contact-mediated renewal produce very different patterns. To understand the origin of these distinct pattern

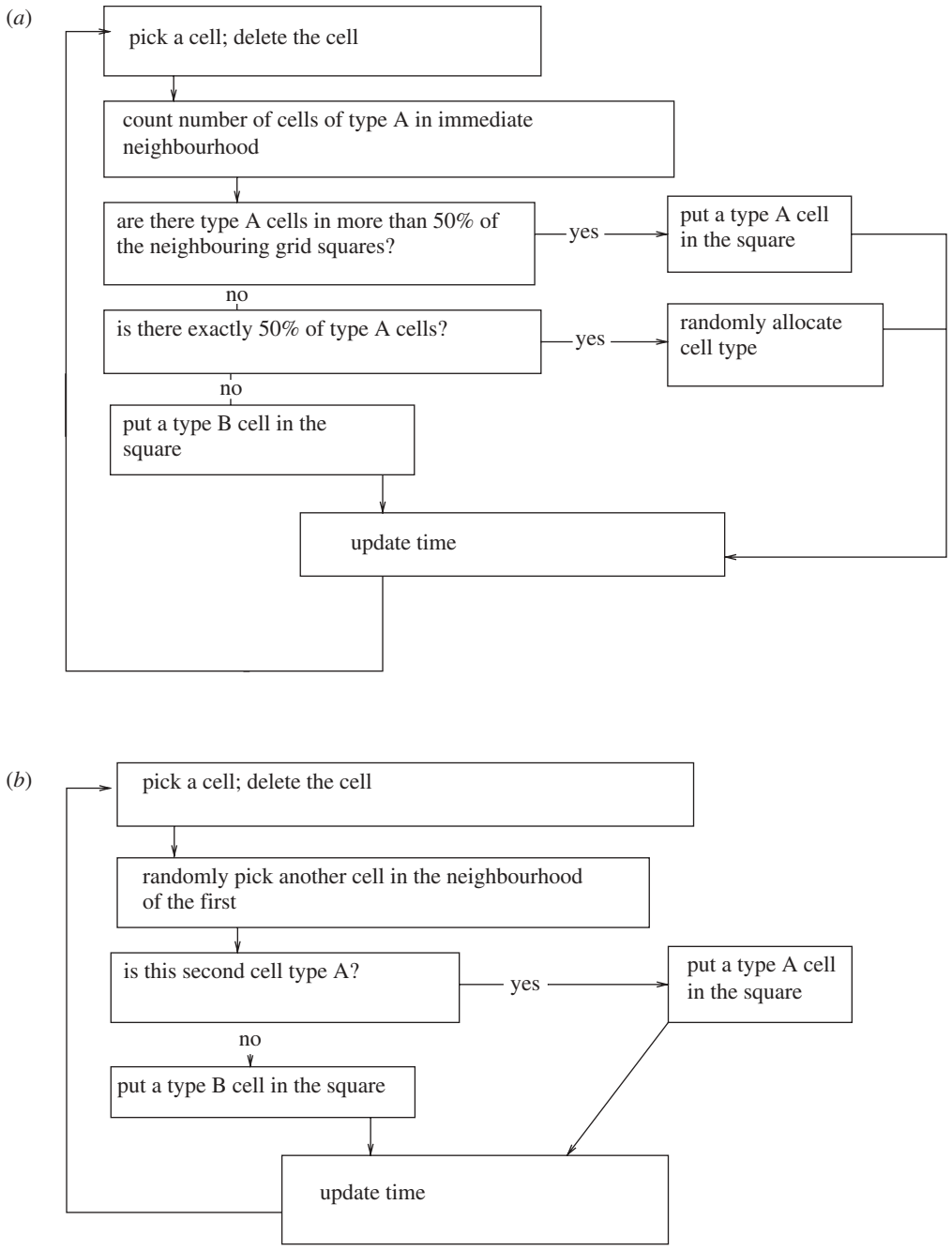

Figure 1. The updating process for the asynchronously updated cellular automata. (*a*) Description of the process for the CA based on the majority conceptual model, while (*b*) describes that of the CA based on the single-cell conceptual model.

outcomes, we develop a continuous framework that is more amenable to mathematical analysis.

2.2. Development of a continuous model

To model our problem continuously, we must decide how to represent the local environment of cells that influence cell renewal. We first use an integral term I to calculate the proportion of one cell type in the local environment, and then apply various functions f to this integral to explore different renewal scenarios. Such a representation of cell environment via an integral term has been used previously in contexts including cell sorting (Armstrong *et al.* 2006), development (Armstrong *et al.* 2009; Green *et al.* submitted) and cancer (Gerisch & Chaplain 2008; Sherratt *et al.* 2009; Painter *et al.* in press). Since we again wish to model a monolayer of cells, the integral I is in two dimensions, and is taken over a region dictated by a sensing radius R, representing the capacity of a cell to directly sense its environment via, for example, filopodial contact. Increasing R allows us to consider different sizes of the neighbourhood that influences cell renewal, and therefore allows us to consider different types of cell communication. For example, a small R can represent contact-dependent communication such as juxtacrine signalling (Owen *et al.* 1999; Webb & Owen 2004), whilst a larger R may be chosen to explore a longer range communication such as a locally diffusing signalling molecule (Monk 1997).

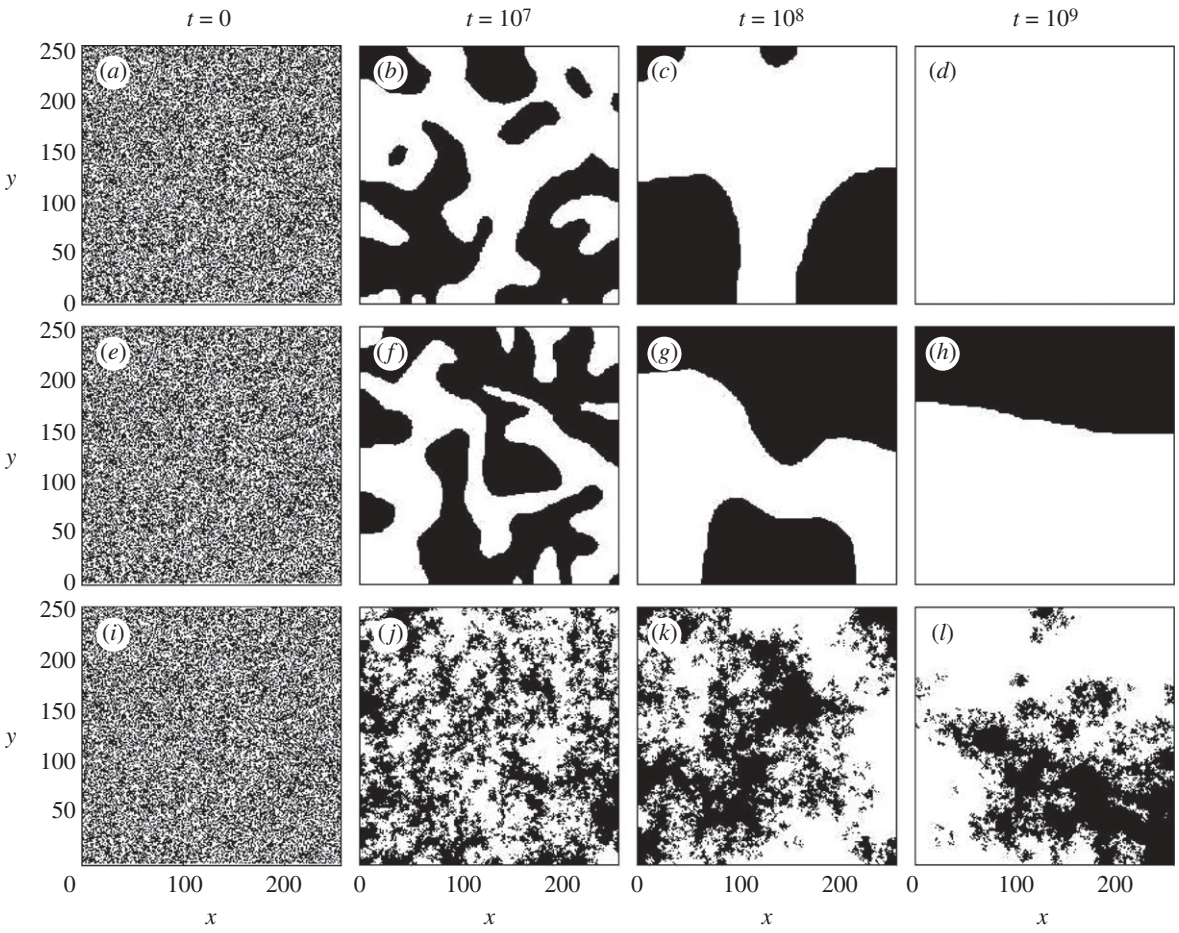

Figure 2. Solution of the cellular automata (CA) as described above, at times $t = 0$, 10^7, 10^8 and 10^9. Here, we use mixed initial conditions by randomly assigning to each grid square the value of 0 or 1. In $(a–d)$ left to right, we consider the majority conceptual model, and see cells quickly forming large agglomerations, before they either die out completely or dominate the grid. Out of 1000 runs, we see quick domination by a single cell type across the entire domain in about 30% of cases, while the remaining 70% end with both species present as seen in $(e–h)$. In $(i–l)$, a solution to the single-cell conceptual model is shown, demonstrating persistence of both cell lines over time. For $(a–d)$ and $(e–h)$, cells are updated according to the process described in figure 1*a*, while the CA in $(i–l)$ is updated according to the process described in figure 1*b*. All CAs are carried out on a grid of size 256×256, and use an eight-neighbour Moore neighbourhood. On the boundary and at the corners of the domain, only cells in the domain are considered, and an average is taken over that reduced number of cells in the majority model, whilst in the single-cell model a cell that picks a neighbour outside the domain does not change state.

Since we are concerned with modelling chimaera experiments, we have a closed system where the birth of cells simply replaces those cells lost to death, i.e. there is no empty space. We further assume that the replacement rates of the two cell lines are the same, as expected in mosaic tissues. This enables the model to be formulated as a single equation for the proportion of cells that are of one of the two types. We refer to the two cell types as A and B, with $a(\underline{x}, t)$ being the proportion of cells of type A; thus a fraction $1 - a(\underline{x}, t)$ of the cells are of type B.

Our complete model is therefore:

$$\frac{\partial a}{\partial t} = \alpha(f(I_a) - a), \tag{2.1}$$

where I_a is the integral $(1/\text{area}) \int_0^R \int_0^{2\pi} a(\underline{x} + r\underline{\eta}) r \, \mathrm{d}\theta \, \mathrm{d}r$. Other cells within the domain of integration in I_a are located relative to $a(\underline{x}, t)$ by reference to both the distance r along the sensing radius R, and $\underline{\eta} = (\cos\theta, \sin\theta)$. The constant α is the cell replacement rate. In terms of the CA model, α is related to the time step since it regulates the rate at which the cell population changes through time. A more accurate relationship could be obtained if a more formal link between the two models was attempted, but as we are primarily interested in the long-term dynamics of the model, and not its rate of change, we do not attempt to derive such a link here. The integral is normalized over the area, which is πR^2 away from the boundaries of the domain. We assume a finite sheet of cells, and hence on the boundary the integral is truncated, i.e. cells that lie outside the domain are not included in our calculations, neither in the integral itself, nor in the calculation of area over which the integral is normalized.

We now consider two different scenarios that explore different local environment dependencies, and that match our CA simulations and conceptual models.

—Locally biased model

(i) Renewal is biased towards the cell type in the local majority.

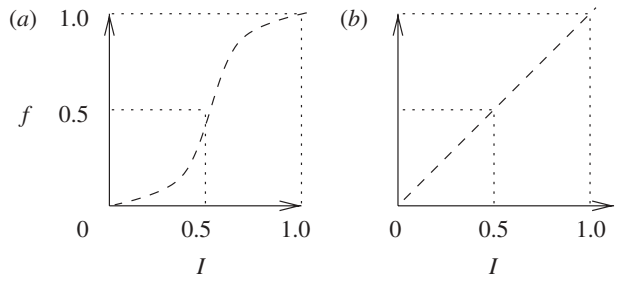

Figure 3. Schematic of renewal function in the continuous model. (*a*) A smooth continuous approximation to a step function, symmetric about $\frac{1}{2}$, representing the locally biased model. (*b*) Linear *f*, representing the locally unbiased model.

(ii) This is equivalent to the majority conceptual model and corresponding CA simulation.
(iii) We choose *f* as illustrated in figure 3*a*: a cell will be replaced with a type biased towards those in the majority around it, in a scenario that mimics that of the community effect witnessed in cell differentiation (see Standley *et al.* 2001).

—Locally unbiased model
(i) Renewal is non-biased.
(ii) This is equivalent to the single-cell conceptual model and CA simulation.
(iii) We choose *f* as illustrated in figure 3*b*: a daughter cell will be of a certain type with a probability equal to the proportion of that cell type present, corresponding to basic cell proliferation.

Note that a must lie between 0 and 1 since it is a proportion, and moreover $f(0) = 0$ and $f(1) = 1$ since both $a = 0$ and 1 must be steady states.

2.3. Linear stability analysis of homogeneous steady states

In order to explore the long-term behaviour we can expect from the model, we carry out some analysis, looking at the location and stability of steady states. Significant steady states of the locally biased model, found by setting $\partial a/\partial t = 0$ in equation (2.1), are given by $a = 0$, $\frac{1}{2}$ and 1. We then perturb the steady states homogeneously through space to explore their stability: we put $a = a_s + \tilde{a}(t)$, where a_s is our steady state and $\tilde{a}$ is a small homogeneous perturbation. Then

$$\frac{\partial \tilde{a}}{\partial t} = \alpha(f(I_{a_s+\tilde{a}}) - (a_s + \tilde{a})). \tag{2.2}$$

At $a_s = 0$ and $a_s = 1$, $f'(I_{a_s}) < 0$, while at $a_s = \frac{1}{2}$, $f'(I_{a_s}) > 0$. Therefore $a = 0$ and 1 are stable, while $a = \frac{1}{2}$ is unstable. For the locally biased model, we therefore expect only one scenario: depending on the initial proportion of A, we expect that the system will always evolve to either all A or all B.

In the same manner, we explore the locally unbiased model. Here there is a continuum of steady states at $a = a_s$, with any $a_s \in [0,1]$ possible. The steady states are neutrally stable. This means we expect the system to remain at whatever proportion of A and B it begins with, which is consistent with the simulations in figure 2*i–l*.

Table 1. A summary table of stability of the steady states of equation (2.1).

model type	steady state	stability
locally biased	0	stable
	$\frac{1}{2}$	unstable
	1	stable
locally unbiased	$a_s \in [0,1]$	neutral

This analysis of the two variations of the model (see table 1 for a summary) suggests that a cell's reaction to its local environment can significantly alter the patterns we can expect to see. With the locally biased version of the model we expect locally to see all cells having a single type, either A or B, whereas in the locally unbiased model we expect to see a persistence of both cell lines. This is consistent with the proliferation hypothesis for the development of organ parenchymas, which suggested that proliferation was the driver behind the creation of differing mosaic patterns (see §1).

3. NUMERICAL SIMULATIONS OF THE CONTINUUM MODELS

Whilst the linear analysis provides some insight into the expected model behaviour, a numerical study is required for further understanding. Our numerical code discretizes the circular domain of the integral, and then sums the integral over each of the grid squares within the circle. Although some of the area of the circle is lost at the boundaries, the calculation is fast and, with a fine lattice, it is reasonably accurate; note that simulations with a reduced lattice give the same qualitative behaviour. More sophisticated numerical schemes for integrodifferential equations using techniques such as fast Fourier transforms to evaluate the integral are possible: see in particular Gerisch & Chaplain (2008) and Gerisch (2010). To discretize time, we used ROWMAP (Weiner *et al.* 1997), a method that is particularly suited to solving stiff ODE initial value problems, and that automatically controls and adjusts time-step size.

3.1. The two-dimensional model results

We begin by investigating initial conditions corresponding to a homogeneous, equal mix of cell types A and B across the grid, so that we set $a = 0.5 \pm$ small noise (see figure 4). This is a biologically realistic scenario for a group of cells at the start of a chimaera experiment. These initial conditions also allow comparisons with our CA simulations. Note that in preliminary investigations, we have found that varying the amplitude of noise present in the initial conditions makes no qualitative difference to the results. We carry out all simulations on a two-dimensional grid with boundary conditions equivalent to the biological scenario of a

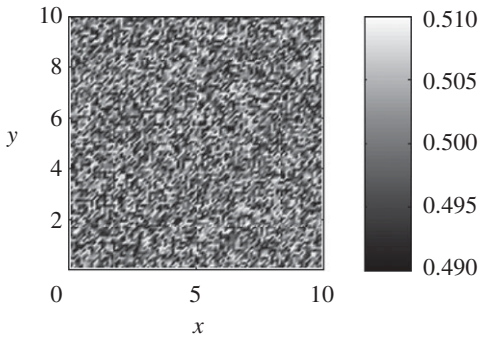

Figure 4. The homogeneous mixed initial conditions used for the two-dimensional model. The two cells are evenly mixed across the domain. The domain is a square with sides of length 10 dimensionless space units.

chimaera experiment: we imagine a sheet of cells with no cells present outside the boundary.

For the locally biased model, we find that the solution usually goes to all A or all B across the entire domain, as expected from our linear analysis (see §2.3). However, sometimes the long-term solution involves a division of the domain into two parts, one solely of type A, and the other solely of type B (figure 5). This occurred in a total of six out of 20 runs. Note that these results are qualitatively the same as those seen in the CA model, but not quantitatively so (see §2.1 and figure 2). However, increasing the gradient of f, moving it closer towards a step-function, causes an increase in the number of times the long-term solution evolves to a domain of one part A and one part B. Intuitively this is not surprising, as in moving f closer to a step function we move closer to the discrete CA scenario in which 70 per cent of our simulations ended with both cell populations present. For the locally unbiased model, we see the two cell populations A and B merge into a single homogeneous state (figure 6). This suggests that biologically, the two cell lines will persist over time alongside one another (corresponding to $b = 1 - a$ with $0 < a < 1$ in equation (2.1)). This result is also similar to our CA simulations for the single-cell contact scenario (see §2.1 and figure 2*i*–*l*), although the continuous model loses the fine-grained spatial dynamics of the discrete model (not shown).

Biologically, solutions of the type shown in figure 5 are reminiscent of the growth patterns of both the adrenal cortex, which involve large blocks of a single cell type alongside one another, and the liver, which involves random patterning. For certain domain sizes our simulations of the locally biased model show repeated stripes, as is seen in the adrenal cortex (see figure 7; note that in this figure, we deliberately use a long, thin domain to encourage stripe formation). These stripes are stable to spatial perturbations, suggesting that something similar to locally biased proliferation could be the driver for the dynamics seen in this organ, although there is no concrete evidence on whether or not this is the case. Moreover, the similarity between our discrete simulations and the patterns observed *in vivo*, along with the continuous model results also showing cell line persistence, suggests that the growth of liver parenchyma may be driven by the cell renewal process as described in the locally unbiased model, although again there is no empirical evidence to confirm this suggestion. In §4, we suggest possible future experiments to test this prediction.

Overall, the result of the locally unbiased model in comparison to that of the locally biased model shows that by merely changing the influence of the local environment on the renewal term, two very different results are observed. This suggests that the way cells react to and communicate with their local environment has a very significant role in the dynamics of homoeostasis.

3.2. Extending the two-dimensional results

We now consider three further sets of initial conditions, in order to gain insight into the behaviours discussed above. In §3.1, the locally biased model sometimes resulted in a split domain. In order to investigate this phenomenon further, we repeat our experiments, this time starting with split conditions similar to those seen in figure 5*l* (see figure 8*a*). With such initial conditions, the interface between the two species does not move over long times, suggesting that we are indeed at a steady state (not shown). Furthermore, we repeat our experiments with a curved interface (see figure 8*b*) in order to discover whether a non-flat interface could cause movement due to mean curvature. We see a flattening of the interface (see figure 9), but no further movement. This coincides with the previous result, and leads us to conclude that a coexistence steady state in the locally biased model will always display a flat interface between the two species. Finally, we investigate 'island' initial conditions (see figure 8*c*), in order to explore the dynamics of a localized group of cells. Again, we see movement driven by mean curvature, i.e. movement is fastest where curvature is greatest. This leads to the 'island' rapidly shrinking until it disappears (see figure 10), explaining both why we sometimes see the dominance of a single species in the locally biased model, and why we do not see spotted patterns, as each small group of cells is engulfed by the larger local population (see figure 5*c*,*g*).[1] While further investigation of curved boundaries and their movement is not the focus of the present paper, it is a natural area for future work, building on the literature of the movement of 'islands' in the two-dimensional Ginzburg–Landau equation, a generic balanced, bistable partial differential equation (Rougemont 2000).

4. DISCUSSION

The results of our mathematical models are consistent with biological experiments, and suggest that the way a cell reacts to its local environment has a significant part to play in cellular patterning in mosaics. Our key finding is that a small change in the reaction to the local cellular environment can produce a very different

[1]Note that such a test was repeated with the majority conceptual CA, and led to the same results (not shown).

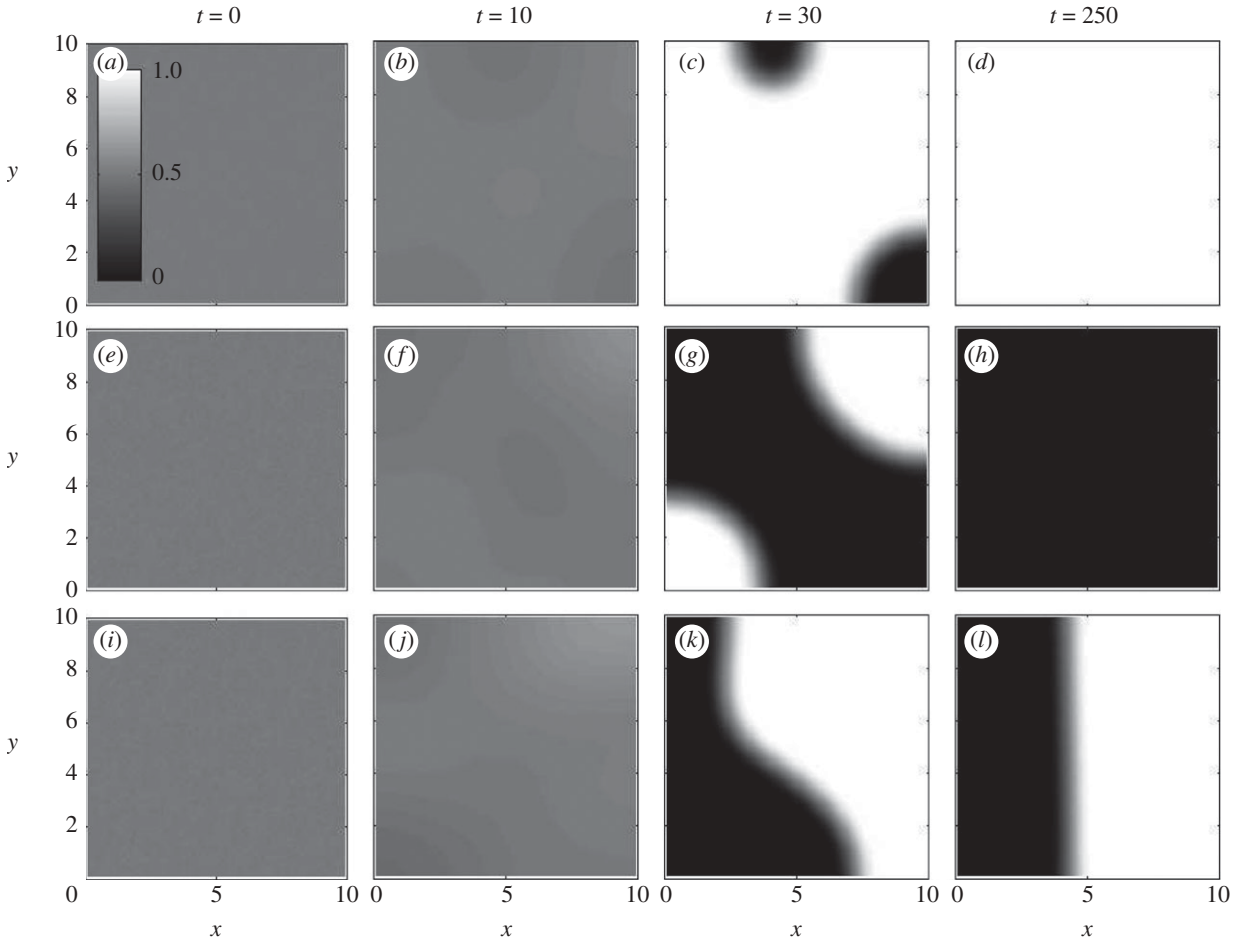

Figure 5. A solution of the two-dimensional locally biased model equations (2.1) with homogeneous initial conditions. We plot the proportion of cells of type A in space at dimensionless times $t = 0$, 10, 30 and 250. (a–d) The domain quickly evolves to an all white domain of A cells; (e–h) quick dominance by B (black). (i–l) Dominance by neither cell type, which held for long times (solutions were found to be stable in runs up to $t = 10^8$; not shown). Out of 20 runs, A dominated 10 times, B 4 times, and neither 6 times. We begin with initial conditions of $a = 0.5 + 0.02 \times c$ where c is chosen randomly between 0 and 1 at each numerical grid point. In (a–d) and (e–h) the function f is given by $f(I) = 0.5 \tanh(\tan(I\pi - 0.5\pi)) + 0.5$, a continuous approximation to a step function, while $f = I$ in (i–l). The dimensionless parameter values are $R = 1.0$, $\alpha = 1.0$. The domain is of size 10 dimensionless space units. We set absolute error tolerance in the ROWMAP scheme to 10^{-6}.

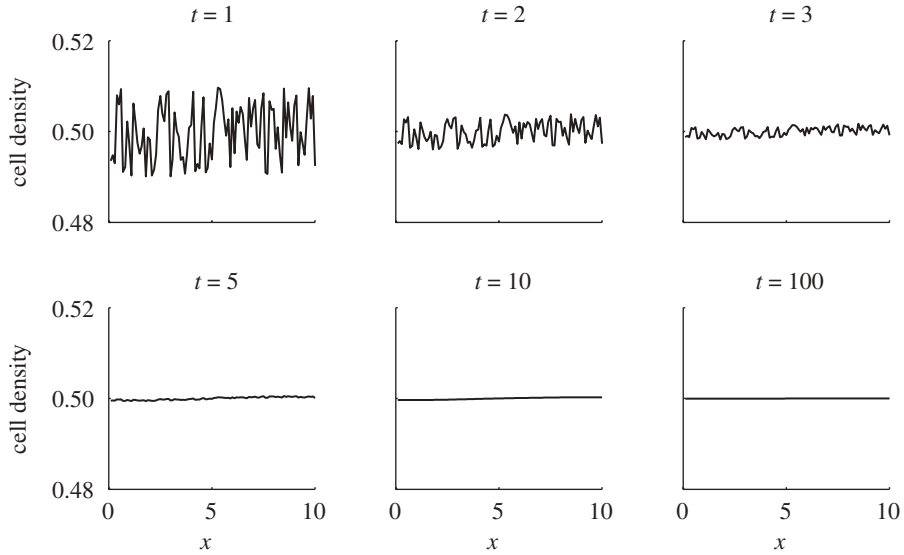

Figure 6. Time evolution plots of the two-dimensional locally unbiased model equations (2.1). The domain is initially an even mix of the cell populations A and B, as in figure 4, and is of size 10 dimensionless space units. We plot the proportion of cell type A across space in the x direction for $y = 2$ at various times t, until $t = 100$. We see the proportion of A spreading homogeneously across the domain over time until $A = 0.5$ everywhere. All parameter values and numerical details are as in figure 5, although with a linear f as stipulated by this model (see figure 3*b*).

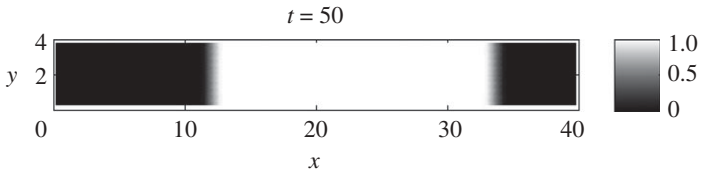

Figure 7. A solution of the two-dimensional locally biased model equations (2.1) with mixed homogeneous initial conditions. We plot the proportion of cells of type A in space at dimensionless time $t = 50$. We see the formation of stable stripes. The domain is 40 dimensionless space units wide, and 4 high. All other numerical details are as in figure 5.

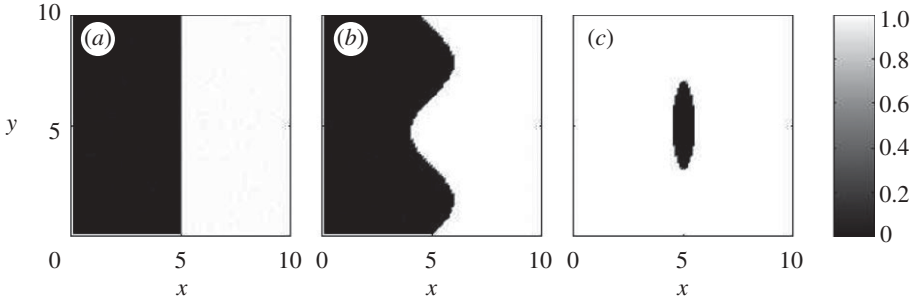

Figure 8. More initial conditions (i.c.s) used for the two-dimensional model. The domain is again a square with sides of length 10 dimensionless space units. (*a*) Split i.c.s, (*b*) curved i.c.s and (*c*) island i.c.s.

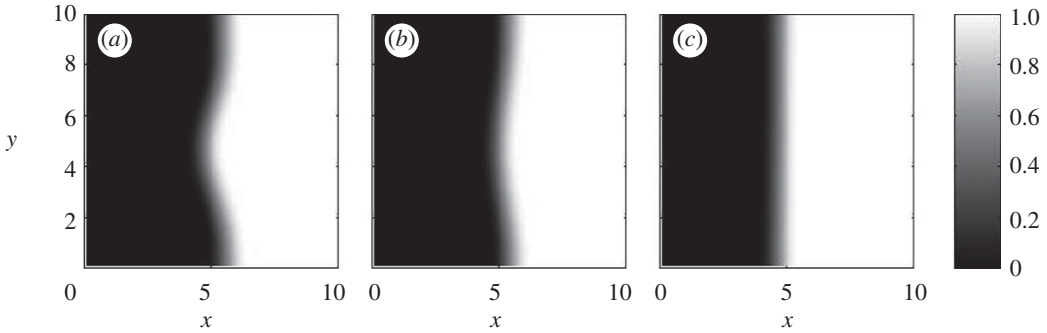

Figure 9. Solutions to the two-dimensional locally biased model equations (2.1) with curved initial conditions as in figure 8*b*. We plot the density of cells in space at (*a*) $t = 10$, (*b*) $t = 20$ and (*c*) $t = 1000$. Neither cell type dominates over long times. All numerical details and parameter values are as in figure 5.

outcome for the overall composition of the tissue. In cell renewal, proliferation of each cell type may depend linearly or nonlinearly on the local proportion of cells of that type, and these two possibilities produce very different patterns. Moreover, by looking at the results of chimaera experiments that explored rat livers and adrenal cortices, we have found that the proliferation hypothesis previously discussed in Simpson *et al.* (2006) and Landini & Iannaccone (2000; see §1), could indeed offer an accurate description of the mechanisms that drive organ parenchyma maintenance, with the different patterns seen being caused by different reactions to cellular contact. If the hypothesis is correct, we predict that cells in the liver renew according to the linear locally unbiased mechanism, and cells in the adrenal cortex renew according to the non-linear Locally Biased mechanism. This is something that could be tested with the use of fluorescent markers: by marking and following mosaic cells from cell lines of various organs *in vitro* and taking regular images of them, one could discover whether cells are renewing according to the locally biased or locally unbiased mechanisms, or according to a different mechanism altogether.

In §1, we discussed the phenomenon of X-chromosome inactivation mosaicism in females, and the hypothesis that the appearance of Blaschko lines in mammals may be related to the patterned placement of activated and inactivated X-chromosomes in the skin (Happle 2006). In the majority of females, cells with one or other X-inactivated chromosome appear mixed evenly across the skin in a fine mosaic (Asplund *et al.* 2001), as is suggested by the locally unbiased model. This model is an effective represention of the proliferation of a single daughter cell from one mother cell, as occurs in normal cell proliferation. This suggests that the patterns created by lesions that occur along Blaschko lines in females could be governed by an interruption of normal proliferation processes. This could cause the different cell lines to appear in large

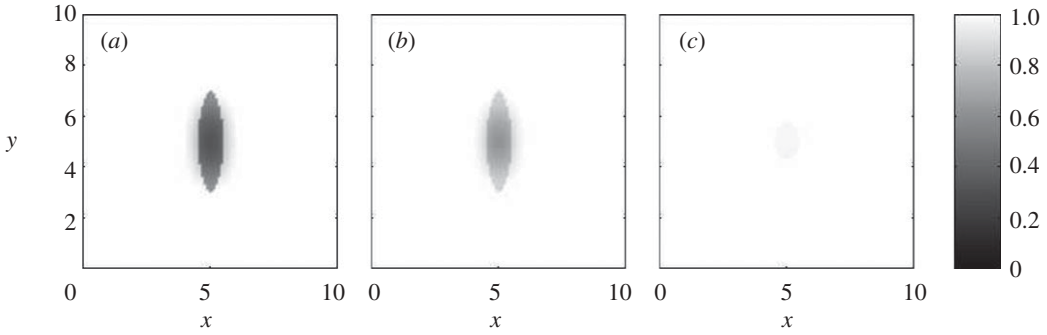

Figure 10. Solutions to the two-dimensional locally biased model equations (2.1) with island initial conditions as in figure 8*c*. We plot the density of cells in space at (*a*) $t = 1$, (*b*) $t = 2$ and (*c*) $t = 5$. The dominant cell type rapidly engulfs the 'island', demonstrating that we will not see spotted patterns. All numerical details and parameter values are as in figure 5.

blocks alongside each other with merging of the two cell lines across their boundary, as is seen in the locally biased model (see figures 5, 7 and 9). Again, experiments could be done with fluorescent markers to see whether this is the case. However, the issue of what could make such a change occur in the normal proliferation process remains to be explored.

Future theoretical work may involve analysing heterogeneous steady states to explore the structure and scale of patterns. This would enable us to investigate more fully the spatial aspects of, for example, the stripe patterns of adrenal cortex chimaeras. We could also investigate more fully different proliferation functions f to represent other possible cell contact scenarios, in order to explore the different patterns seen in various organs in chimaera experiments. Extending the model to three dimensions would allow much better comparisons with experimental work, as currently most of the quantitative results gathered from chimaeras is in the form of two-dimensional sections from three-dimensional tissues. Considering the corresponding model on a growing domain would also allow more precise comparisons. In a similar vein, one could attempt a continuous model that is more closely derived from a discrete model. The parameters in a discrete model can in some cases be reliably estimated from microscopic data, and thus could then be used to estimate parameters in the macroscopic model. One possible method of deriving a continuous model would be to consider the probabilities of a cell in the CA becoming type A, say, over a large number of realizations, and to use the variance as a basis for the function f in the continuous model. We have not attempted such a derivation as we do not have the precise biological data that would be required to make the link between the model types of real value. However, this step would be useful in the creation of a three-dimensional model for which there are good microscopic data available.

Our model could also be extended to explore scenarios that are outside the closed system necessitated by chimaera experiments. As it stands, the continuum model could be used to study the role of community effects in cell differentiation, and we plan to apply the model to this cellular process in the near future. A variation of the model may also be used to explore more general cell proliferation: this would require a factor of a being included in the proliferation term of equation (2.1). Such an amended model would explicitly relate the total population of one cell type to the proliferation rate of that cell type, and would allow us to consider growing cell populations. However, for the particular application we have considered, our rather different renewal term is appropriate, and the resulting model has highlighted the importance of correct formulation in exploring the tissue dynamics arising from cellular renewal.

J. M. Bloomfield was supported by a Doctoral Training Account Studentship from EPSRC. K. J. Painter and J. A. Sherratt were supported in part by Integrative Cancer Biology Program Grant CA113004 from the US National Institute of Health, and in part by BBSRC and EPSRC funding to the Centre for Systems Biology at Edinburgh. J. A. Sherratt was supported in part by a Leverhulme Trust Research Fellowship. G. Landini was supported in part by STFC Grant ST/F003404/1.

REFERENCES

Anderson, A. R. A., Chaplain, M. A. J. & Rejniak, K. A. 2007 *Single-cell-based models in biology and medicine.* New York, NY: Springer.

Armstrong, N. J., Painter, K. J. & Sherratt, J. A. 2006 A continuum approach to modelling cell–cell adhesion. *J. Theor. Biol.* **243**, 98–113. (doi:10.1016/j.jtbi.2006.05.030)

Armstrong, N. J., Painter, K. J. & Sherratt, J. A. 2009 Adding adhesion to the cell cycle model for somite formation. *Bull. Math. Biol.* **71**, 1–24. (doi:10.1007/s11538-008-9350-1)

Asplund, A., Guo, Z., Hu, X., Wassberg, C. & Ponten, F. 2001 Mosaic pattern of maternal and paternal keratinocyte clones in normal human epidermis revelaed by analysis of X-chromosome inactivation. *J. Invest. Derm.* **117**, 128–131. (doi:10.1046/j.0022-202x.2001.01385.x)

Cox, J. T. & Durrett, R. 1991 Nonlinear Voter Models. In *Random walks, Brownian motion, and interacting particle systems* (eds R. Durrett & H. Kesten), pp 189–202. Boston, MA: Birkhäuser.

Cox, J. T. & Griffeath, D. 1986 Diffusive clustering in the two dimensional voter model. *Ann. Probab.* **14**, 347–370. (doi:10.1214/aop/1176992521)

Dornic, I., Chaté, H., Chave, J. & Hinrichsen, H. 2001 Critical coarsening without surface tension: the universality class of the voter model. *Phys. Rev. Lett.* **87**, 045701. (doi:10.1103/PhysRevLett.87.045701)

Gerisch, A. 2010 On the approximation and efficient evaluation of integral terms in PDE models of cell adhesion. *IMAJ. Numer. Anal.* **30**, 173–194. (doi:10.1093/imanum/drp027)

Gerisch, A. & Chaplain, M. 2008 Mathematical modelling of cancer cell invasion of tissue: local and non-local models and the effect of adhesion. *J. Theor. Biol.* **250**, 684–704. (doi:10.1016/j.jtbi.2007.10.026)

Graham, B. & van Ooyen, A. 2006 Mathematical modelling and numerical simulation of the morphological development of neurons. *BMC Neurol.* **7** (Suppl. 1), S9. (doi:10.1186/1471-2202-7-S1-S9)

Green, J. E. F., Waters, S. L., Shakesheff, K. M., Edelstein-Keshet, L. & Byrne, H. M. Submitted. Non-local models for the interactions of hepatocytes and stellate cells during aggregation.

Happle, R. 2006 X-chromosome inactivation: role in skin disease expression. *Act. Paedia.* **95**, 16–23. (doi:10.1080/08035320600618775)

Iannaccone, P. M. & Weinberg, W. C. 1987 The histogenesis of the rat adrenal cortex: a study based on histological analysis of mosaic pattern in chimeras. *J. Exp. Zool.* **243**, 217–223. (doi:10.1002/jez.1402430207)

Iannaccone, P., Morley, S., Skimina, T., Mullins, J. & Landini, G. 2002 Cord-like mosaic patches in the adrenal cortex are fractal: implications for growth and development. *FASEB.* (doi:10.1096/fj02-0451fje)

Khokha, M. K., Landini, G. & Iannaccone, P. M. 1994 Fractal geometry in rat chimeras demonstrates that a repetitive cell division program may generate liver parenchyma. *Dev. Biol.* **165**, 545–555. (doi:10.1006/dbio.1994.1274)

Landini, G. & Iannaccone, P. M. 2000 Modelling of mosaic patterns in chimeric liver and adrenal cortex: algorithmic organogenesis? *FASEB* **14**, 823–827.

Liggett, T. M. 1985 *Interacting particle systems*. New York, NY: Springer.

Lyon, M. 1961 Gene action in the X-chromosome of the mouse. *Nature* **190**, 372–373. (doi:10.1038/190372a0)

Monk, N. A. M. 1997 The community effect and ectoderm–mesoderm interaction in *Xenopus* muscle differentiation. *Bull. Math. Biol.* **59**, 409–425.

Morley, S. D., Viard, I., Chung, B.-C., Ikeda, Y., Parker, K. L. & Mullins, J. J. 1996 Variegated expression of a mouse steroid 21-hydroxylase/beta-galactosidase transgene suggests centripetal migration of adrenocortical cells. *Mol. Endo.* **10**, 585–598. (doi:10.1210/me.10.5.585)

Murray, J. D. 1989 *Mathematical biology*, vol. 1, 3rd edn. New York, NY: Springer.

Ng, Y. K. & Iannaccone, P. M. 1992 Experimental chimeras: current concepts and controversies in normal development and pathogenesis. *Curr. Top. Dev. Biol.* **27**, 235–274. (doi:10.1016/S0070-2153(08)60536-0)

Owen, M. R., Sherratt, J. A. & Myers, S. R. 1999 How far can a juxtacrine signal travel? *Proc. R. Soc. Lond. B* **266**, 579–585. (doi:10.1098/rspb.1999.0675)

Painter, K. J., Armstrong, N. J. & Sherratt, J. A. In press. The impact of adhesion on cellular invasion processes in cancer and development. *J. Theor. Biol.* (doi:10.1016/j.jtbi.2010.03.033)

Rougemont, J. 2000. Evaporation of droplets in the two-dimensional Ginzburg-Landau equation. *Physica D* **140**, 267–282. (doi:10.1016/S0167-2789(00)00009-9)

Schönfisch, B. & de Roos, A. 1999 Synchronous and asynchronous updating in cellular automata. *BioSystems* **51**, 123–143. (doi:10.1016/S0303-2647(99)00025-8)

Sherratt, J. A., Armstrong, N. J., Gourley, S. J. & Painter, K. J. 2009 Boundedness of solutions of a nonlocal reaction–diffusion model for cellular adhesion. *Eur. J. Appl. Math.* **20**, 123–144. (doi:10.1017/S0956792508007742)

Simpson, M. J., Landman, K. A., Hughes, B. D. & Newgreen, D. F. 2006 Looking inside an invasion wave of cells using continuum models: Proliferation is the key. *J. Theor. Biol.* **243**, 343–360. (doi:10.1016/j.jtbi.2006.06.021)

Simpson, M. J., Merrifield, A., Landman, K. A. & Hughes, B. D. 2007*a* Simulating invasion with cellular automata: connecting cell-scale and population-scale properties. *Phys. Rev. E* **76**, 021918. (doi:10.1103/PhysRevE.76.021918)

Simpson, M. J., Zhang, D. C., Mariani, M., Landman, K. A. & Newgreen, D. F. 2007*b* Cell proliferation drives neural crest cell invasion of the intestine. *Dev. Biol.* **302**, 553–568. (doi:10.1016/j.ydbio.2006.10.017)

Standley, H. J., Zorn, A. M. & Gurdon, J. B. 2001 eFGF and its mode of action in the community effect during Xenopus myogenesis. *Development* **128**, 1347–1357.

Webb, S. D. & Owen, M. R. 2004 Intra-membrane ligand diffusion and cell shape modulate juxtacrine patterning. *J. Theor. Biol.* **230**, 99–117. (doi:10.1016/j.jtbi.2004.04.024)

Weiner, R., Schmitt, B. A. & Podhaisky, H. 1997 ROWMAP—a ROW-code with Krylov techniques for large stiff ODEs. *Appl. Numer. Math.* **25**, 303–319. (doi:10.1016/S0168-9274(97)00067-6)

West, J. D. 1998 Insights into Development and Genetics from Mouse Chimeras. In *Current Topics in Developmental Biology*, vol. 44 (eds R. A. Pedersen & G. P. Schatten), pp. 21–67. San Diego, CA: Academic Press.